

A novel method to compare tropospheric path delay fluctuations with 22-GHz water vapor line emissions

Yoshiharu Asaki^a, Hideyuki Kobayashi^b, Naoki Hagiwara^c, and
Masato Ishiguro^d

^aInstitute of Space and Astronautical Science, 3-1-1 Yoshinodai, Sagamihara, Kanagawa, Japan

^bNational Astronomical Observatory, Osawa, Mitaka, Tokyo, Japan

^cUniversity of Electro-Communications, Tyohugaoka, Tyohu, Tokyo, Japan

^dNobeyama Radio Observatory, Nobayama, Minamimaki, Minamisaku, Nagano, Japan

ABSTRACT

Tropospheric phase fluctuation due to the water vapor content is one of difficult problems which degrades imaging performances of radio interferometry. One of the potential solutions is differential radiometry observations to measure the differential water vapor content along the line of sights. We developed a 22-GHz-line radiometer to be mounted on a ground data-link antenna which supplies the timing reference signal for a space VLBI satellite, HALCA. This system will allow us to compare directly the atmospheric phase fluctuation with the water vapor content along a single line of sight measured by the radiometer.

Keywords: atmospheric phase fluctuation, interferometry, water vapor

1. INTRODUCTION

Tropospheric phase fluctuation due to the water vapor content limits imaging performances of millimeter- and submillimeter-wave interferometer arrays and VLBI. There are a few kinds of techniques which have been proposed and applied for correcting the atmospheric phase fluctuation, such as the fast antenna switching method,¹ the paired antenna method,^{2,3} and the differential radiometric method.⁴

As one of the method, the differential radiometric phase correction has been used for the interferometric phase correction by use of a correlation between the fluctuation of the excess path length (EPL) and the brightness temperature of the water vapor radio emission.⁵ A radiometer is mounted on a radio telescope to measure the amount of the water vapor along the line of sight. This method is considered as a potential technique to correct the phase errors in radio interferometry.^{6,7}

To apply the radiometric phase correction, we must know a conversion factor to transfer the brightness temperature of the water vapor to the degree of the fringe phase shift at the observing frequency. Although the conversion factor can be obtained using theoretical models,^{5,8} the relation of the conversion factor with an elevation angle or weather conditions at an antenna site is not well understood.

The Institute of Space and Astronautical Science (ISAS) launched an astronomical satellite named “HALCA” in February 1997. The satellite was carried into an elliptical orbit to be dedicated to international space VLBI experiments. Since the frequency standard of HALCA is transmitted up from a ground tracking station, the round-trip phase back to the tracking station fluctuates due to the atmosphere. This means that the atmospheric phase fluctuation of the single EPL can be studied by using the phase transfer system between HALCA and the tracking stations. If a radiometer is mounted on the tracking antenna, we can investigate the direct relation between the tropospheric path delay and water vapor emission at varying elevation angles and weather conditions. So this phase transfer system can provide a unique experimental tool to measure tropospheric phase delay along a single line of sight.⁹

Further author information: (Send correspondence to Y.Asaki)

Y.Asaki: E-mail: asaki@vsop.isas.ac.jp

H.Kobayashi: E-mail: hkobaya@hotaka.mtk.nao.ac.jp

N.Hagiwara: E-mail: naoki@hotaka.mtk.nao.ac.jp

M.Ishiguro: E-mail: ishiguro@nro.nao.ac.jp

In this report, we describe a novel method to compare the tropospheric phase fluctuation with 22-GHz water vapor line emission along a single line of sight. In Section 2, we introduce HALCA and its phase transfer system. Section 3 outlines the basic relation of the radiometric phase correction. A 22-GHz line radiometer developed is also described in Section 3. Summary is given in Section 4.

2. A ROUND-TRIP PHASE TRANSFER FOR “HALCA”

In February 1997, ISAS launched HALCA, which has a deployable 8-m radio telescope to observe celestial sources at 1.6 and 5 GHz. HALCA has been operated by the VLBI Space Observatory Program (VSOP) with many organizations and ground radio telescopes around the world.¹⁰ Space VLBI observations with HALCA can extend an interferometric baseline up to three times longer than the earth’s diameter.

2.1. Principles of the phase transfer system

For VLBI observations, a highly stable frequency reference is needed such as an atomic maser standards. As HALCA does not have any on-board frequency standards, the reference signal is supplied as an up-link carrier from one of five tracking stations in the world: three of the Deep Space Network (DSN) stations of the National Aeronautics and Space Administration (NASA), one at the National Radio Astronomy Observatory (NRAO) in Green Bank, and one by ISAS at Usuda, Japan. The up-link signal for the phase transfer is generated from a hydrogen maser frequency standard at each tracking station and transmitted at a nominal 15.3 GHz, although the up-link frequency is controlled at the tracking station to compensate for the spacecraft Doppler shift due to the orbital motion.

Reference signals on the satellite for down-converting and sampling celestial signals are all generated from the up-link signal. The digitized data at 128 Mbps is mixed with a carrier at 14.2 GHz and modulated with Quadrature Phase Shift Keying (QPSK). The astronomical data is transmitted back to the tracking station as a down-link signal with no Doppler compensation at the satellite. Figures 1 and 2 show the phase transfer system schematics and block diagrams, respectively.

2.2. Phase instability in the round-trip system

The round-trip phase of the phase transfer system is affected by the Doppler shift and the turbulent atmosphere.¹¹ The top plots in Figure 3 show phase instability observed in the round-trip phase obtained at the Usuda tracking station after compensation of the Doppler shift. The bottom plots show the root temporal structure function $\sqrt{\bar{D}_\Phi(T)}$, defined by

$$\bar{D}_\Phi(T) \equiv \langle \{\Phi(t+T) - \Phi(t)\}^2 \rangle, \quad (1)$$

where t is time, Φ is a half of the round-trip phase (one way) at 15.3 GHz, and T is the sampling interval.¹² For the tropospheric turbulence, a combination of Kolmogorov’s theory and a frozen-flow hypothesis¹² shows that,

$$\bar{D}_\Phi(T) \propto T^\alpha, \quad (2)$$

where α is called structure exponent. Typical values for the structure exponent are 5/3, 2/3, and 0 for $T < 100$ sec, $100 \leq T < 1000$ sec, and $T \geq 1000$ sec, respectively. The exponents of the sampling interval less than 20 sec of each plot are 1.34, 1.60, and 1.42 for May 1 and 27, 1997, and February 27, 1998, respectively, while the Kolmogorov theory predicts 5/3. Although the exponents are rather flatter than the prediction, we can see the characteristics of the atmospheric phase fluctuation, such as the turning point of the exponent.^{13,14}

Let us consider the ionospheric effects to the phase transfer. The ionospheric excess delay τ_i is given by

$$\tau_i = \frac{40.3}{cf^2} \times TEC, \quad (3)$$

where c is the light velocity, f is the transmitted frequency, TEC is *total electron content*.⁵ Assuming TEC is $6.03 \times 10^{17} \text{ m}^{-2}$ in the mid day time, the ionospheric delay is 347 picosec at 15.3 GHz. The scintillation index, SI , is calculated as follows,

$$SI = \frac{\sigma_{\tau_i}}{\tau_i}, \quad (4)$$

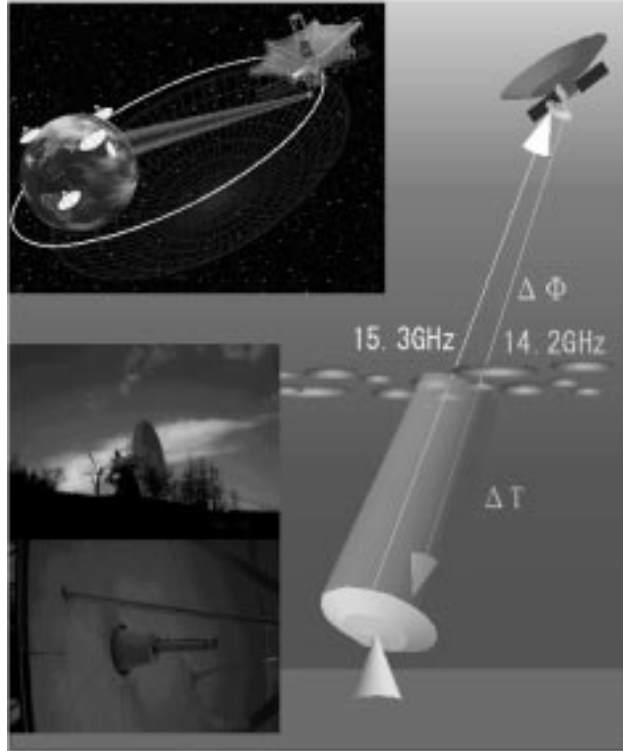


Figure 1. Schematic drawings of the phase transfer system between HALCA and the tracking stations. At the lower left is the 10-m antenna of the tracking station at Usuda, Japan.

where σ_{τ_i} is the rms ionospheric fluctuation. A relation between the rms fluctuation and Allan standard deviation $\sigma_y(\tau)$ is

$$\sigma_y(\tau) = \frac{3\sigma_{\tau_i} T_L}{4\pi^2 \tau^2}, \quad (5)$$

where τ is a sampling interval, and T_L is the lowest cut off period of the fluctuation. Assuming SI of 0.1 and T_L of 0.1 sec, the stability of the ionospheric delay for an averaging time of 1 sec is calculated as 0.26 picosec/sec. This value is almost comparable to the stability of the transponder of HALCA and one order of magnitude less than the atmospheric phase fluctuation.¹¹ So we consider that the ionospheric phase fluctuation is negligible compared with the tropospheric phase fluctuation.

3. WATER VAPOR LINE RADIOMETER

3.1. Basic relations

From the radiative transfer equation, the sky brightness temperature T_B is given by

$$T_B = T_{atm}(1 - e^{-\tau}), \quad (6)$$

where T_{atm} and τ are the physical temperature and opacity of the atmosphere, respectively. With an assumption that $\tau \ll 1$, we obtain

$$T_B = \tau T_{atm}. \quad (7)$$

Here, τ consists of contributions due to the dry air τ_d , water vapor τ_w , and a liquid component τ_l ,

$$\tau = \tau_d + \tau_w + \tau_l. \quad (8)$$

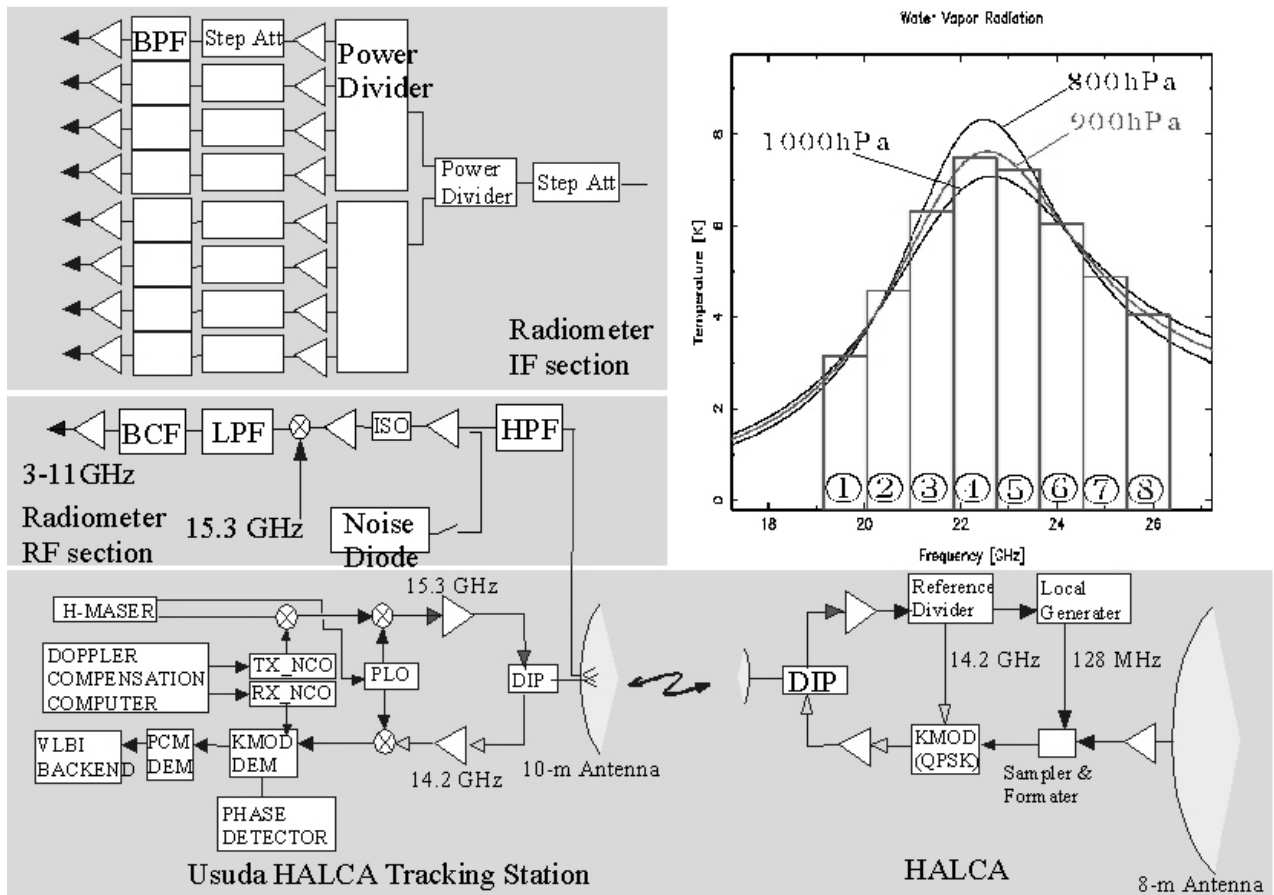


Figure 2. Block diagrams of the phase transfer system between HALCA and the Usuda tracking station (lower panel), and the 22-GHz line radiometer (upper left panels). At the upper right, the expected water vapor line shape at the Usuda station and our frequency channelization, covering 19.15 to 26.35 GHz.

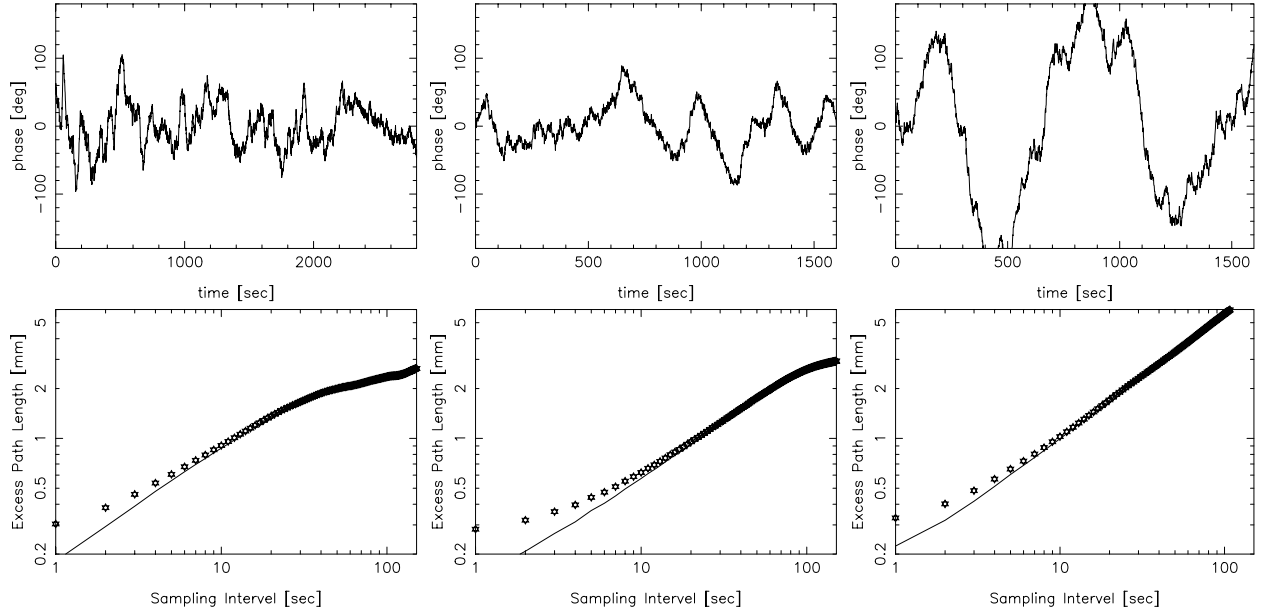


Figure 3. Phase instability in the HALCA round-trip phase measured at the Usuda tracking station. The top plots are time variations of the half of the round-trip phase adjusted to 15.3 GHz on May 1 and 27, 1997, and February 27, 1998. Bottom, the temporal structure functions. Note that the ordinate is the excess path length (EPL) in millimeters. Solid lines are calculated assuming a system noise of 4.5° for 0.1-sec averaging. The slope of the temporal structure functions at smaller sampling intervals are 0.67, 0.80, and 0.71 for May 1 and 27, 1997, and February 27, 1998, respectively.

The liquid component does not contribute to EPL. While the dry component does, it is well mixed and does not cause time variation. The distribution of the water vapor is spatially not-well-mixed and time-variable. This leads to the EPL fluctuation in the atmosphere, which causes the fluctuation of fringe phase.

The water vapor emission peaks at 22.235 GHz. The line shape is broadened by the atmospheric pressure as shown in Figure 2. Dual-frequency radiometers (24 and 31 GHz) are widely used aiming to remove the contribution of the liquid component; while this method successfully measures the water vapor content under clear sky, the correlation between the interferometer phase shift and the brightness temperature measured tends to break under cloudy sky. Line radiometers covering 18–26 GHz successfully show the correlation even under cloudy sky.^{7,15}

3.2. Instruments

The radiometer developed consists of two sections as shown in Figure 2. Received signals at 19.15–26.35 GHz are amplified with a low noise amplifier (LNA) in the RF section. Since, in tracking HALCA, the link antenna transmits the 15.3-GHz up-link signal of 14 dBm, there can be a possibility to cause saturation of the LNA. Therefore, a wave-guide-type high pass filter with the cut off frequency of 16 GHz is inserted in the front of the LNA. Gain calibration is carried out by referring to the equivalent noise temperature of a noise diode inserted just in front of the LNA through a -20 -dB coupler. To reduce the LNA gain drift and equivalent temperature fluctuation of the noise diode, the RF section is temperature-stabilized with thermic heaters. The received signal is down-converted to 3.85–11.05 GHz and transmitted to the IF section to be fed into eight 900-MHz-wide frequency channels to obtain the line shape of the water vapor emission. The frequencies are listed in Table 1 with the equivalent receiver noise temperatures.

The radiometer is designed to be mounted close to the Cassegrain focus of the 10-m dish of the Usuda tracking station in order to illuminate the sub reflector as shown in Figure 4. The offset angle of the line of sight of the radiometer from the beam of the tracking antenna is 0.6° , which corresponds to a spatial distance of 11 m at 1-km height. Assuming that a wind velocity above is 10 m/s, the duration of the transverse distance is nearly 1 sec. This



Figure 4. The 22-GHz line radiometer mounted on the 10-m dish of the Usuda tracking station.

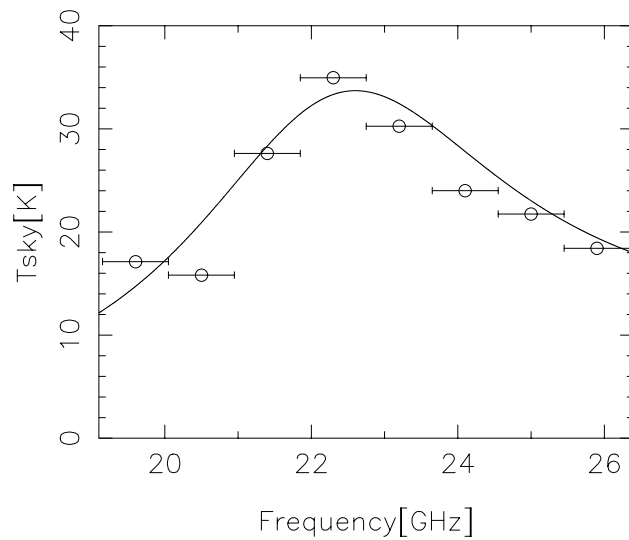


Figure 5. A spectrum of the sky brightness temperature measured with the line radiometer. A solid line represents an expected line shape of the atmosphere obtained from theoretical models. Each bar shows a frequency coverage of each channel of the radiometer.

effect can be negligible to compare the round-trip phase and the brightness temperature by adopting an averaging time greater than a few seconds.

3.3. Preliminary results

We have conducted preliminary measurements with the line radiometer. Figure 5 shows a measured spectrum of the sky brightness temperature. In these observations, the radiometer was set on the ground to observe the zenith direction. The time variation of the brightness difference obtained by $T_{sky4} - (T_{sky1} + T_{sky8})/2$ is shown in Figure

Table 1. Frequency table of the water vapor line radiometer.

Channel	Frequency (GHz)	Receiver Noise Temperature (K°)
1	19.15 – 20.05	219.2
2	20.05 – 20.95	226.3
3	20.95 – 21.85	216.5
4	21.85 – 22.75	193.1
5	22.75 – 23.65	207.5
6	23.65 – 24.55	227.3
7	24.55 – 25.45	230.6
8	25.45 – 26.35	245.3

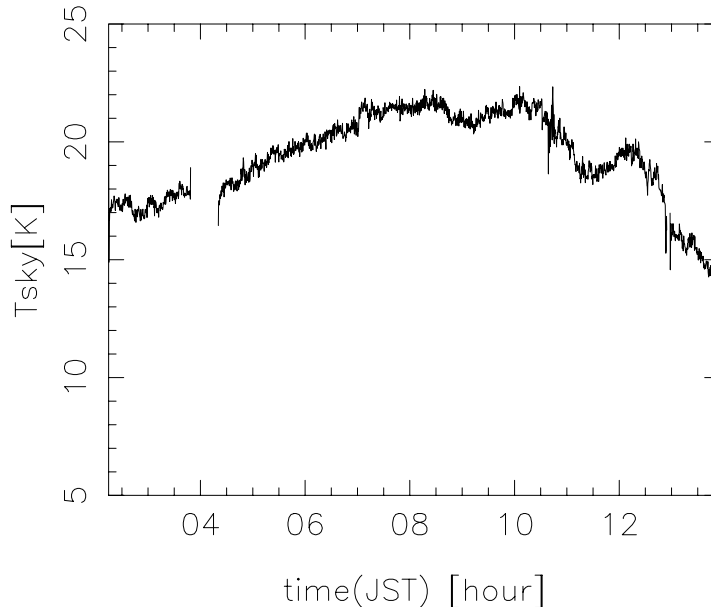


Figure 6. Time variation of the relative brightness temperature.

6, where T_{sky1} , T_{sky4} , and T_{sky8} are the sky brightness temperatures of the frequency channels 1, 4, and 8. The averaging of channels 1 and 8 is “off” the water vapor line emission, while channel 4 is “on”. The peak height corresponding to the amount of the water vapor content will be determined by fitting the measured data to the theoretical models.

4. SUMMARY

A 22-GHz water line radiometer was developed to be mounted at the focus of the Usuda 10-m antenna. The radiometer was designed to have eight frequency channels covering 19.15 to 26.35 GHz with 900 MHz bandwidth each to measure the line profile of the water vapor emission with the peak at 22.235 GHz. With this method, we can investigate the direct relation between the tropospheric path delay fluctuation and water vapor line emission at various elevation angles and weather conditions. The hardware for the radiometer has been completed and will be mounted on the Usuda tracking antenna in April, 2000.

ACKNOWLEDGMENTS

The authors wish to express their gratitude to N. Kawaguchi of National Astronomical Observatory of Japan for his suggestion and guidance, and H. Shimomura and K. Ohgi of Nihon Tsushinki Corporation for the integration of the instrument.

REFERENCES

1. C. L. Carilli and M. A. Holdaway, "Tropospheric phase calibration in millimeter interferometry," *Radio Sci.* **34**, pp. 817–840, 1999.
2. Y. Asaki, M. Saito, R. Kawabe, K.-I. Morita, and T. Sasao, "Phase compensation experiments with the paired antennas method," *Radio Sci.* **31**, pp. 1615–1625, 1996.
3. Y. Asaki, K. M. Shibata, R. Kawabe, D. G. Roh, M. Saito, K.-I. Morita, and T. Sasao, "Phase compensation experiments with the paired antennas method 2, millimeter wave fringe correction using a centimeter wave reference," *Radio Sci.* **33**, pp. 1297–1318, 1998.
4. G. M. Resch, D. E. Hogg, and P. J. Napier, "Radiometric correction of atmospheric path length fluctuations in interferometric experiments," *Radio Sci.* **19**, pp. 411–422, 1984.
5. A. Thompson, J. Moran, and G. Swenson, *Interferometry and Synthesis in Radio Astronomy*, A Wiley-Interscience publication, New York, 1986.
6. M. Bremer, S. Guilloteau, and R. Lucas, "Atmospheric phase correction based on sky emission in the 210–248 GHz band," in *Science with Large Millimeter Arrays*, P. Shaver, ed., vol. 3357, pp. 240–246, 1997.
7. K. B. Marvel and D. P. Wooday, "Phase correction at millimeter wavelengths using observations of water vapor at 22 GHz," in *Advanced Technology MMW, Radio, and Terahertz Telescopes held at Hawaii*, I. G. Phillips, ed., *Proc. SPIE* **3357**, pp. 442–452, 1998.
8. H. J. Liebe, "An updated model for millimeter wave propagation in moist air," *Radio Sci.* **20**, pp. 1069–1089, 1985.
9. M. Ishiguro, N. Kawaguchi, Y. Asaki, and H. Hirose, "A novel method to compare the tropospheric path delay fluctuations with 22 GHz water vapor line emissions," *Abstracts of General Assembly of URSI XXVI*, p. 844, 1999.
10. H. Hirabayashi, H. Hirose, H. Kobayashi, Y. Murata, P. G. Edwards, E. B. Fomalont, K. Fujisawa, T. Ichikawa, T. Kii, J. E. Lovell, G. A. Moellenbrock, R. Okayasu, M. Inoue, N. Kawaguchi, S. Kamenoi, K. M. Shibata, Y. Asaki, T. Bushimata, S. Enome, S. Horiuchi, T. Miyaji, T. Umemoto, V. Migenes, K. Wajima, J. Nakajima, M. Morimoto, J. Ellis, D. L. Meier, D. W. Murphy, R. A. Preston, J. G. Smith, S. J. Tingay, D. L. Traub, R. D. Wietfeldt, J. M. Benson, M. J. Claussen, C. Flatters, J. D. Romney, J. S. Ulvestad, L. R. D'Addario, G. I. Langston, A. H. Minter, B. R. Carlson, P. E. Dewdney, D. L. Jauncey, J. E. Reynolds, A. R. Taylor, P. M. McCulloch, W. H. Cannon, L. I. Gurvits, A. J. Mioduszewski, and R. T. Schilizzi, "Overview and initial results of the very long baseline interferometry space observatory programme on radio interferometric measurements," *Science* **281**, pp. 1825–1829, 1998.
11. N. Kawaguchi, *New VLBI Observing Techniques under Strong Atmospheric Fluctuations*, The graduated university for advanced studies, Kanagawa, Japan, 1998.
12. V. I. Tatarskii, *Wave Propagation in a Turbulent Medium*, Dover, New York, 1961.
13. R. N. Treuhaft and G. E. Lanyi, "The effect of the dynamic wet troposphere on radio interferometric measurements," *Radio Sci.* **22**, pp. 251–265, 1987.
14. A. F. Dravskikh and A. M. Finkelstein, "Tropospheric limitations in phase and frequency coordinate measurements in astronomy," *Radio Sci.* **60**, pp. 251–265, 1979.
15. D. A. Tahmouh and A. E. E. Rogers, "Frequency switching wvrs for tropospheric path delay correction," *Abstracts of General Assembly of URSI XXVI*, p. 843, 1999.